Accurate Spectral Characterization of Polarization-Dependent Loss

R. M. Craig

Abstract—**Building on previous work, a rapid automated nonmechanical measurement system for spectral characterization of polarization-dependent loss (PDL) has been developed. A deterministic fixed-states Mueller–Stokes method in conjunction with realtime calibrated spectral information is used to derive wavelength-dependent Mueller matrix elements. Voltage-modulated liquid-crystal variable retarders set the input polarization states. A narrow voltage-tuned filter provides a wavelength sweep following a broadband source; the sweep wavelength is calibrated in realtime by hydrogen cyanide reference lines. This rapid measurement system can measure PDL over a wavelength range of 15 nm in 5 s. A complete uncertainty analysis has been conducted for PDL in the range of 0.05 to 0.3 dB with an expanded uncertainty of 0.0098 dB over the range of 1535 to 1560 nm. Performance was verified using a Fresnel reference. Finally, design and performance results from all-fiber artifact calibration standards are presented.**

Index Terms—**Low coherence, Mueller-matrix, polarization-dependent loss (PDL), wavelength dependence.**

I. Introduction

UNTIL THE advent of dense wavelength-division multiplexing (DWDM) systems, polarization-dependent loss (PDL) was usually characterized at only a specific wavelength [1]. More recently, however, the wavelength dependence of PDL [PDL(λ)] has assumed greater importance [2], particularly in component metrology. A modification of a previously reported deterministic fixed-states technique [3] has been implemented that allows PDL to be accurately characterized as a function of wavelength in this system. The goal is to establish a capability for rapid measurement of PDL(λ) to a standard uncertainty less than 0.005 dB without sacrificing accuracy. This approach uses a nonmechanical matrix technique employing ratio detection and simultaneous spectral calibration via a hydrogen cyanide reference (HCN) that is faster than most tunable-laser systems (taking only 5 s for a 15 nm range) and more accurate than optical spectrum analyzer-based techniques [4]. In addition, this approach can be customized to the resolution requirements of both wideband and narrow-band devices. Wideband devices, e.g., switches, commonly exhibit a small variation in PDL(λ) that does not require a fine wavelength resolution. In contrast, a narrow-band or -channel device such as a filter may exhibit relatively small values of PDL(λ) over the transmission (or reflection) band but large values at the band edge. This type of device requires higher wavelength resolution for accurate characterization.

Manuscript received March 27, 2002; revised November 1, 2002.

The author is with the National Institute of Standards, and Technology, Boulder, CO 80305 USA.

Digital Object Identifier 10.1109/JLT.2003.808761

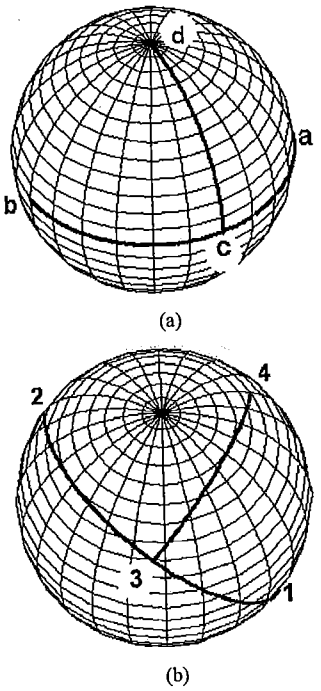

Fig. 1. (a) Initial Poincaré sphere trajectories of the LCVR state generators. (b) LCVR trajectories following birefringent displacement.

New results from an all-fiber PDL(λ) artifact reference are also presented. This artifact is a National Institute of Standards and Technology (NIST), Boulder, CO, measurement assurance program (MAP) transfer standard with PDL values in the range of 0.05–0.3 dB for the calibration of measurement instrumentation.

In Section II, the concept of the measurement method is discussed, and Section III describes the experimental implementation. Section IV outlines a comprehensive uncertainty analysis.

II. Concept

Our method is a further variation of a matrix technique, sometimes referred to as the Mueller–Stokes technique, developed by Favin *et al.* [5], [6] and modified by Craig *et al.* [3]. The method relies solely on measurements of power ratio at specific polarization states, but it has now been extended to accurately cover a range of wavelengths. As in [3], four well-defined polarization states are necessary to determine the first-row Mueller matrix elements of a component. Diattenuation, the global polarization dependence of transmittance, can be determined from these (wavelength-dependent) matrix elements. Because the measurement depends only on the relative coordinates of the four states,

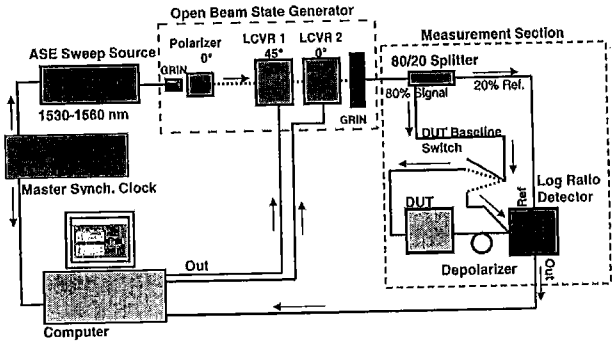

Fig. 2. Simplified diagram of the measurement system.

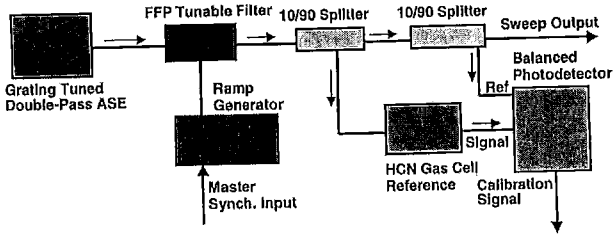

Fig. 3. Diagram of swept-wavelength source with HCN calibrator (sweep source).

the sole requirements on the set are that they maintain relative angular separations of 90° (orthogonality) about the origin of the polarization Poincaré sphere, as shown in Fig. 1. Thus, any constant retardance in the measurement path will not affect the measured PDL since pure retardance does not alter the orthogonality of the states but merely rotates them uniformly on the sphere. Measurement system PDL in conjunction with retardance, however, modifies this scenario somewhat by altering the relationship between the launched states and can potentially introduce significant uncertainty. This uncertainty and its resolution will be discussed in detail in Section IV.

In the Mueller–Stokes technique, PDL is measured by launching four orthogonal polarization states into the device-under-test (DUT) and for each state, measuring the ratio of the transmitted power $[I_{T1}(\lambda)\ldots I_{T4}(\lambda)]$ to the launched power $[I_{L1}(\lambda)\ldots I_{L4}(\lambda)]$. Including the wavelength dependence of these powers, the first row of Mueller matrix elements can be defined from [3] as

$$\begin{bmatrix} m_{11}(\lambda) \\ m_{12}(\lambda) \\ m_{13}(\lambda) \\ m_{14}(\lambda) \end{bmatrix} = \begin{bmatrix} \frac{1}{2}\left[\frac{I_{T1}(\lambda)}{I_{L1}(\lambda)} + \frac{I_{T2}(\lambda)}{I_{L2}(\lambda)}\right] \\ \frac{1}{2}\left[\frac{I_{T1}(\lambda)}{I_{L1}(\lambda)} - \frac{I_{T2}(\lambda)}{I_{L2}(\lambda)}\right] \\ -\frac{1}{2}\left[\frac{I_{T1}(\lambda)}{I_{L1}(\lambda)} + \frac{I_{T2}(\lambda)}{I_{L2}(\lambda)}\right] + \frac{I_{T3}(\lambda)}{I_{L3}(\lambda)} \\ -\frac{1}{2}\left[\frac{I_{T1}(\lambda)}{I_{L1}(\lambda)} + \frac{I_{T2}(\lambda)}{I_{L2}(\lambda)}\right] + \frac{I_{T4}(\lambda)}{I_{L4}(\lambda)} \end{bmatrix}. \quad (1)$$

The spectral transmittance extrema $T_{\min}(\lambda)$ and $T_{\max}(\lambda)$ are obtained from the previous matrix elements by optimization as

$$\begin{aligned} T_{\max}(\lambda) &= m_{11}(\lambda) + \sqrt{m_{12}(\lambda)^2 + m_{13}(\lambda)^2 + m_{14}(\lambda)^2} \\ T_{\min}(\lambda) &= m_{11}(\lambda) - \sqrt{m_{12}(\lambda)^2 + m_{13}(\lambda)^2 + m_{14}(\lambda)^2} \end{aligned} \quad (2)$$

so that

$$\mathrm{PDL}_\lambda \equiv \mathrm{PDL}(\lambda) = 10\log\left[\frac{\mathrm{T}_{\max}(\lambda)}{\mathrm{T}_{\min}(\lambda)}\right]$$

holds globally over the entire space of polarization states and wavelength.

Errors due to PDL(λ) internal to the measurement system and the wavelength dependence of the liquid-crystal variable retarders (LCVR) are dramatically reduced through normalization of DUT input and output powers in two separate ratios. This arrangement virtually eliminates fluctuations in source power, common-mode drift, spectral dependence in the measurement system, and system PDL(λ). In the first normalization, four initial ratio measurements $I_{T1}(\lambda)\ldots I_{T4}(\lambda)$ are taken that are, in fact, signal-to-reference ratios without the DUT in place, while the final four measurements $I_{L1}(\lambda)\ldots I_{L4}(\lambda)$ are signal-to-reference ratios with the DUT in place. These ratios remove spectral dependence in various elements of the system as well as source fluctuations and common-mode drift. The second normalization is simply the ratio of I_T and I_L as used in (1). This removes the inherent PDL(λ) of the system so that only the PDL(λ) of the DUT remains.

III. Implementation

Fig. 2 shows a schematic of the measurement system. The system consists of three major sections: 1) an amplified, spontaneous-emission (ASE) source with a tunable, filtered output calibrated against a NIST wavelength reference; 2) the LCVR polarization state generator; and 3) a measurement section.

A. Light Source and Wavelength Calibration

The ASE source in Fig. 3 is of a spectrally flattened NIST design followed by a fiber Fabry–Perot tunable filter (FFP-TF) tunable over the ASE range from 1535 – 1560 nm with a full-width-at-half-maximum (FWHM) bandwidth of 0.7 nm and a free-spectral range of 85 nm. The FFP-TF is driven by a ramp-generator circuit in a repetitive sweep that is triggered by signals from the control computer. The FFP-TF output is tapped by two 10/90 wavelength-independent couplers in series. The first directs 10% of the light through a NIST HCN wavelength reference (Standard Reference Material [SRM] 2519) [7] to one input of a balanced differential InGaAs photoreceiver. The second directs 9% of the light to the other input of the differential photoreceiver to act as a source-level reference. The differential photoreceiver produces an HCN absorption spectrum that acts as a calibration signal with 50 dB of common-mode rejection. This calibration signal is sampled to 16-bit resolution by the control computer and logged. The absorption peaks are fitted by a least-squares quadratic fit and compared to the known peak wavelengths following each scan, providing near realtime spectral calibration of each sample point. This calibration signal appears in Fig. 4. Presently, each sweep spans only 15 nm of the range from 1535–1560 nm because of speed and sampling-density constraints related to HCN calibration; a full span of 25 nm must be covered in at least two steps. The 0.7-nm Lorentzian bandwidth $\Delta\lambda$ of the source at $\lambda = 1550$ nm gives a coherence length

$$l_c = \frac{\lambda^2}{\pi\Delta\lambda} \equiv 1.1 \text{ mm}. \quad (3)$$

This coherence length is insignificant compared to the typical distances (of order 1 cm) between uncoated surfaces in the measurement system, so multiple-reflection interference is minimized.

B. Polarization-State Generation

The major portion of the swept-source output light is collimated by a gradient-refractive-index (GRIN) lens and then passed through a Glan–Thompson polarizer followed by a series of two LCVR units used to generate the four polarization states. An LCVR is a liquid crystal element whose retardance can be controlled by an applied voltage. The first LCVR, with fast axis at 45° to the incident polarization provides either zero to half-wave retardance. The second, with fast axis at 0° provides zero or quarter-wave retardance. The combined effect of the changes in retardance is the emulation of both half-wave and quarter-wave bulk elements whose function is to either rotate or circularize the incident linear polarization state. Each shift in retardance is synchronized with a source wavelength sweep so that each state setting triggers a new spectral sweep.

The choice of sweep priority, (i.e., each polarization state having its own wavelength sweep rather than the launching of each of four states at every wavelength of a single spectral sweep) was made because it allows rapid spectral calibration. Each spectral sweep was sampled at a rate sufficient to resolve HCN absorption peaks to the required accuracy. The spectral data for each polarization state are aligned in wavelength. Voltages are generated by the control computer and synchronized to the source sweep by a master clock modulate LCVR retardance. Retardance modulation was checked periodically against a polarimeter to ensure the proper relationship among the four states. After the second LCVR, a pigtailed GRIN lens launches the polarization-modulated light back into single-mode (SM) fiber connected to a spectrally flattened 80/20 splitter.

C. Measurement and Calibration

Transmitted and launched powers were measured, respectively, with and without the DUT in place, cf. Fig. 2. The 80/20 splitter was used followed by a ratio detector to obtain the I_T and I_L ratios to source power (removing effects of drift). The major portion (80%) of the splitter output can be switched between the DUT and a direct connection to the first input of a second balanced differential photoreceiver to establish a measurement baseline. The system calibration is checked by replacing the DUT with a fiber-pigtailed open-beam cavity containing a polished BK-7[1] glass block and a high numerical aperature (NA) multimode (MM) depolarizer. The block can be tilted to vary the Fresnel reflections in a predictable way to emulate a PDL. The high numerical aperture (0.37) of the MM fiber is sufficient to essentially depolarize the signal, thereby reducing measurement uncertainty arising from output connector and detector PDL and producing a more accurate calibration. The photoreceiver detection area is sufficient to eliminate speckle uncertainty. Calculated (Fresnel) and measured PDL(λ) values as a function of input angle are presented in Fig. 5 and agree to ± 0.005 dB. The residual system PDL was measured at 0° (normal incidence) as a 0.0014 ± 0.0006 dB offset over all wavelengths. A residual slope indicates a small systematic uncertainty from the wavelength dependence of the 80/20 splitter since BK7 has negligible dispersion over this range.

[1]The identification is made to adequately describe the experimental procedure and is not an endorsement by the NIST; nor does it imply that the material is the best available for this use.

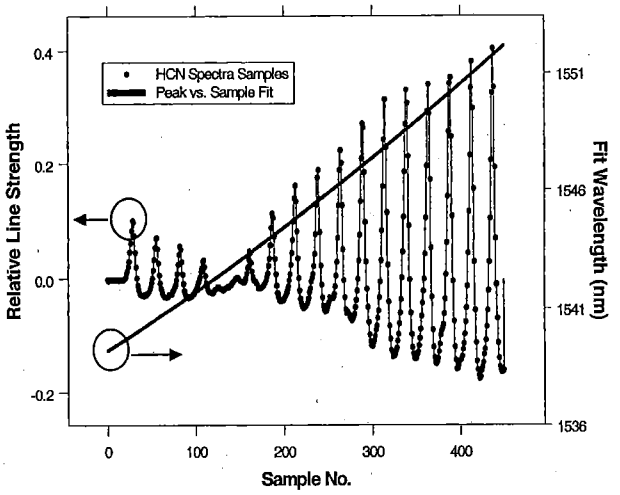

Fig. 4. Typical P-branch HCN absorption signature from 1539 to 1551 nm with a quadratic-calibration fit.

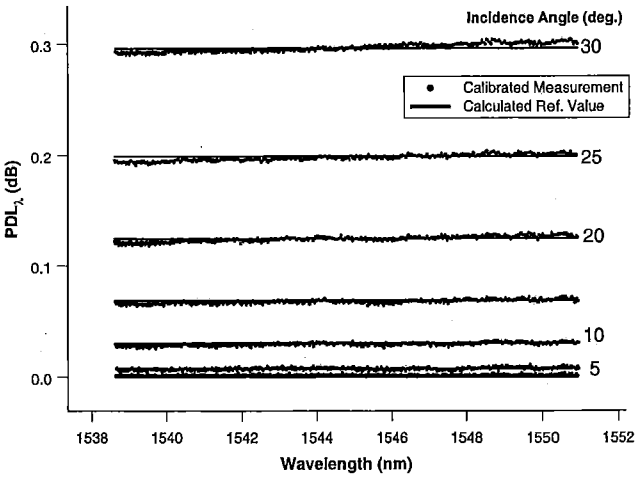

Fig. 5. Open-beam BK7 artifact data calibrated at 30° incidence. Measured and calculated values at other angles of incidence are also shown. Centerline is the calculated PDL(λ) value. Residual wavelength slope falls within 2σ uncertainty.

The DUT PDL(λ) signal was sampled at 450 points for each 15-nm wavelength scan. A scan period of 285 ms was required for each polarization state. A PDL(λ) scan over the entire 15-nm range takes less than 5 s.

IV. Uncertainties

The design of this measurement system is both simpler and more sophisticated than that described in [3] in that taking appropriate ratios of key parameters now reduces most uncertainties. Items 1–4, in the following, outline the four major systematic uncertainties in polarization and power that, together, comprise the total systematic contributions. The remaining

random uncertainties are listed in order of decreasing impact. Values listed correspond to one standard deviation at 1545 nm. The uncertainty analysis is guided by [8].

A. Type B Components [8]

1) Polarization-State Accuracy: Launched polarization states were measured using a polarimeter. Polarization state accuracy depends on both the polarimeter and the LCVR bias calibration. In this case, the polarimeter has been calibrated (open beam) for three linear states and one circular state by means of a 60-dB extinction Glan–Thompson polarizer followed by a NIST quarter-wave retardance reference [9].The retardance reference is certified to 0.1° uncertainty at 1300 nm and has 0.2° uncertainty for low-coherence sources out to 1560 nm. The angular resolution for alignment of these two optical elements is 0.02°, a negligible contribution. The associated contribution to uncertainty is the total calibration uncertainty of all four states generated by the pair. Polarimeter/LCVR system measurements are repeatable to 0.06% (0.1°) over linear state angles and to 0.6% (0.5°) in ellipticity over the Poincaré sphere at 1545 nm. Following the polarimeter calibration, the LCVR bias was adjusted at 1545 nm to match the calibration states to within approximately 2.1%. However, a small systematic offset in the ellipticity of the LCVR circular state of 3.6% remains. The resulting root-sum-of-squares (RSS) PDL standard uncertainty contribution was 1.2% (in dB) for each of the linear states and 2.1% for the circular state.

2) Retarder Wavelength Dependence: The same drive voltage is used on each LCVR state regardless of wavelength, and this causes an uncertainty in the polarization states due to the LCVR wavelength dependence. Based on wavelength-dependent retardance measurements supplied by the vendor, the retardance exhibits only a simple inverse dependence on wavelength λ as $\phi_{\mathrm{VR}} = 2\pi\Phi_\phi(\mathrm{V},\mathrm{T})/\lambda$, where $\Phi_\phi(\mathrm{V},\mathrm{T})$ is the LCVR phase delay (in nm) as a function of voltage V and temperature T. The associated uncertainty contribution is: $(\Delta\phi_{\mathrm{VR}})_\lambda = 2\pi\Phi_\phi(\mathrm{V},\mathrm{T})\,\Delta\lambda/\lambda^2$ where a wavelength scan of $\Delta\lambda = 10$ nm about $\lambda = 1550$ nm produces a normalized standard uncertainty of $\Delta\phi_{\mathrm{VR}}/\phi_{\mathrm{VR}} = 0.35\%$. This uncertainty is manifested primarily as an uncertainty in the accuracy of each Stokes state and its associated matrix element. This uncertainty could be reduced through the use of a look-up table.

3) Retarder Temperature Dependence: The LCVR retardance has an uncertainty due to temperature of $(\Delta\phi_{\mathrm{VR}})_T = (2\pi/\lambda)(\partial\Phi_\phi(\mathrm{V},\mathrm{T})\,\Delta T/\partial T)$, where the vendor's estimate of $\partial\phi_\phi/\partial T$ is 0.004 nm/°C. A temperature variation of 0.5°C (ΔT) gives a normalized standard uncertainty contribution of $(\Delta\phi_{\mathrm{VR}})_T/\phi_{\mathrm{VR}} = 0.12\%$ for our conditions and reflects the temperature uncertainty common in our laboratory during measurements.

4) System Internal PDL Variation: The LCVR elements contribute their own PDL (0.02 dB) to that of the DUT. This manifests itself as a change in intensity with a change in polarization state. This PDL is assumed constant during both phases of the measurement and is cancelled in the normalization ratios. However, any variation in system PDL over the course of a measurement appears as an uncertainty in signal power. Given the maximum observed drift of the internal PDL of 0.02 dB over common measurement intervals of 5 min. This yields a PDL standard uncertainty due to LCVR elements of 0.15%.

Propagated Measurement System Uncertainty: The previous element percentages, inherent to the measurement system, are adjusted standard uncertainties that assume a rectangular distribution [8]. From these values, an error-propagation model based on the definition (1) produces a Type B standard uncertainty of 0.0047 dB at a reference PDL value of 0.12 dB.

B. Type A Components [8]

1) PDL Measurement Repeatability: Effects that can be considered statistical in nature include possible coherent interference at the photoreceiver, calibration-spectral-peak registration uncertainty and resulting fit uncertainty, and photoreceiver noise. The combined effect is encompassed by a measurement of system repeatability. Ten undisturbed measurements of a PDL(λ) for a 0.12 dB BK-7 artifact were made following the initial baseline measurement. The standard deviation of these measurements averaged over all wavelengths yields 0.0012 dB as the effective standard uncertainty of single-sweep system noise and incorporates all effects such as optical interference and detector noise that average down over multiple measurements.

Combined Standard Uncertainty for the Measurement System: The previous Type A and Type B components are assumed uncorrelated, so their root-square-sum (RSS) at the 0.12 dB level is uncertainty of $u_{\mathrm{sys}} = \sqrt{(0.0012^2 + 0.0047^2)}$ dB $= 0.0049$ dB for an open-beam PDL measurement. Using a coverage factor ($k = 2$), the expanded uncertainty [8] follows as $2u_{\mathrm{sys}} = 0.0098$ dB.

C. Type A Artifact Contributions

1) Birefringence-Effect Uncertainty: When measuring devices with significant birefringence in the path (fiber pigtails etc.), the uncertainty associated with four-state measurements has been calculated to be a variation of 4.5% about the mean of measured PDL(λ) in dB. This value is derived from a computer model (to be discussed in a future publication) of four-state measurements in the presence of multiple PDL sources linked by birefringent fiber. Briefly, this effect arises from a shortcoming of the four-state derivation assumptions that neglect the effect of birefringence (e.g., a coiled patchcord) combined with PDL in the measurement system itself. At the 0.12-dB PDL reference value, this uncertainty is 0.0054 dB.

2) Connector Uncertainty: As in [3], a significant source of uncertainty that is not inherent to the LCVR system is variations in measured PDL of DUT artifacts with connectorized pigtails following disconnection and reconnection. This could be explained by connector alignment (core offset) errors. We have measured this uncertainty to be 0.0029 dB/connector-pair for connectorized artifacts. Fusion splicing could reduce this value somewhat.

Combined Standard Uncertainty for the Measurement Artifact: Summing the previous uncorrelated artifact contributions, the total RSS is $u_{\mathrm{DUT}} = \sqrt{(0.0054^2 + 0.0029^2)}$ dB $= 0.0061$ dB at the 0.12-dB level.

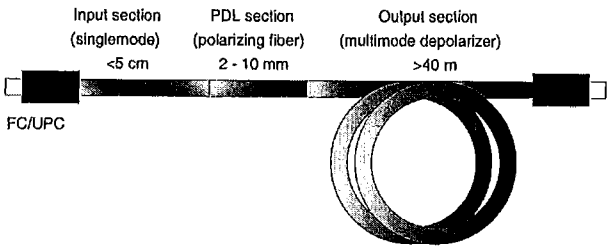

Fig. 6. Simplified schematic of the all-fiber PDL(λ) artifact.

Note that this uncertainty is present in any Mueller-Stokes four-state measurement of PDL.

Total Combined Standard Uncertainty: The RSS total of all previous uncertainty contributions is then

$$u_{MS} = \sqrt{(u_{\text{sys}}^2 + u_{\text{DUT}}^2)} = \sqrt{(0.0049^2 + 0.0061^2)}\ \text{dB} = 0.0079\ \text{dB}$$

which represents the uncertainty in a typical measurement. The expanded uncertainty is then $2u_{MS} = 0.016$ dB.

D. Wavelength Calibration Uncertainty

Based on sampling density, the wavelength uncertainty is estimated to be 0.025 nm for the 0.7-nm FWHM bandwidth of the tunable filter element. For wideband devices in which PDL is constant or varies slowly with wavelength, this uncertainty is not significant. For narrow-band devices such as filters, however, this uncertainty may be significant. This value enters the artifact uncertainty in a product with the slope of PDL(λ).

Stress and thermal drifts in optical-fiber birefringence must be minimized over the course of a measurement. The measurement method is sensitive to small errors in the matrix elements, such as those due to retardance drift between the baseline and DUT measurement. For this reason, one should use short straight leads anchored to a fixed surface and calibrate the system prior to each series of measurements.

V. All-Fiber PDL Artifact Results

A series of all-fiber PDL artifacts has been constructed (Fig. 6) to aid in the establishment of a NIST PDL(λ) transfer standard,. These artifacts consist of three sections: SM, polarizing (PZ), and MM fiber, fusion-spliced together to generate PDL(λ) in the range of 0.05 dB – 0.3 dB over the ITU C-band. The active section consists of 5–10 mm of polarizing fiber (18 dB/m extinction) that provides relatively stable PDL over the range of 15–35 °C. The input is a 5-cm section of single-mode (SMF-28) fiber for accurate coupling to system leads. The output section is composed of 40 m of 50/125 μm step-index multimode fiber of high NA (0.37). The entire length of the splice region is gently immobilized with custom protectors.

This design was chosen initially to provide a simple and relatively inexpensive fabrication method for multiple units. The all-fiber design avoids the usual complications associated with open-beam optics. In practice, one typically trades one set of problems for another. Given the highly stressed

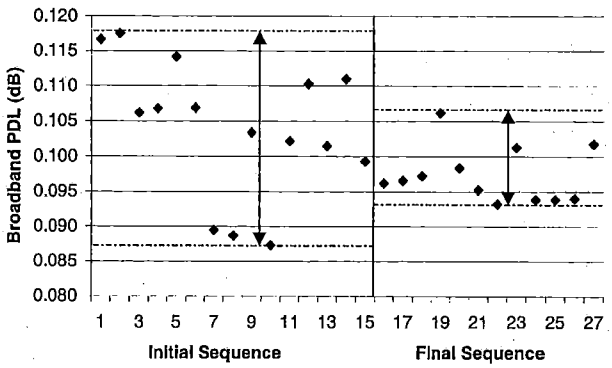

Fig. 7. The "initial sequence" illustrates the thermal instability in artifact PDL before annealing measured with a broad optical source. The "final sequence" illustrates the reduced thermal instability following annealing.

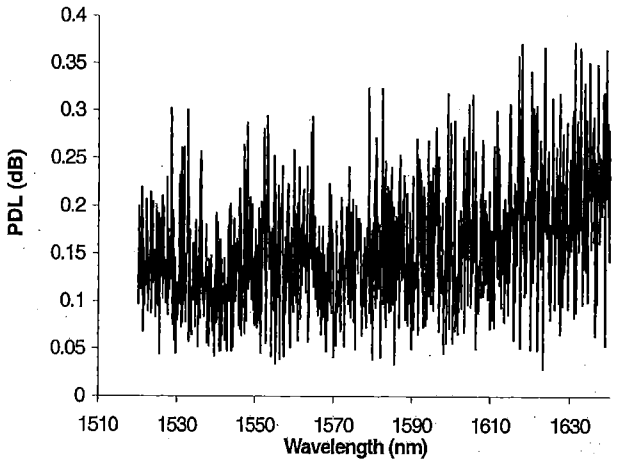

Fig. 8. PDL(λ) data on a 0.1-dB (nominal) artifact taken with a tunable laser source.

nature of polarizing fiber, for example, some sensitivity to variations in the thermal environment can be expected. It was surprising however, to see the magnitude of the variations in PDL with temperature immediately following construction. These variations can easily reach ±80% of the intended value due, presumably, to shifts in the splice protection assembly. With repeated thermal cycling over the temperature range of 0 °C–50 °C, though, thermal movement usually begins to subside and measured PDL begins to stabilize. This behavior is illustrated in Fig. 7. Additional challenges include reliably splicing dissimilar fibers. Fusion splicers that employ electric arcs were found to be particularly troublesome by causing bubbling of the PZ fiber material. A different splicer using hotwire heating was found to produce, with the right parameters, a more consistent and splice of better quality. Another issue is that of back-reflections at the junctions of dissimilar fibers. When dissimilar fibers are joined, there will be back-reflections due to joint imperfections and to Fresnel reflections at the index boundaries, both of which lead to etalon interference when high coherence sources are used to measure PDL. The level of these reflections can be inferred from the observed interference modulation of PDL(λ) as measured with a highly coherent source such as a tunable laser. The magnitude of the modulation, $\Delta\text{PDL}_{\text{mod}}$ (Fig. 8), is approximately 0.25 dB,

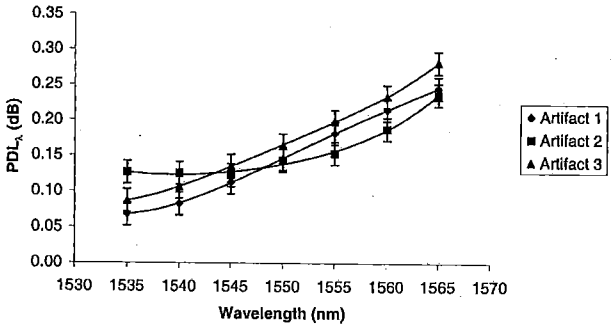

Fig. 9. PDL(λ) measured data and least-squares fit for three artifact prototypes.

which can be equated to the fringe contrast of a simple etalon from

$$\triangle \mathrm{PDL}_{\mathrm{mod}} = 10 \log \left(\frac{(1 - \mathrm{R_j})^2}{(1 - \mathrm{R_j})^2} \right) \tag{4}$$

where R_j is the reflection at each splice joint. Consequently, R_j can be solved to yield a reflection of 1.4% across each joint. This effect precludes the use of these artifacts in measurement systems employing highly coherent sources. In fact, to prevent this effect, one should limit the coherence length L_c to 10% of the PZ fiber length (or $L_c < 1.1$ mm). This coherence length corresponds to a source bandwidth of approximately 0.7 nm (for a source with Lorentzian profile) and is satisfied by our measurement system.

Some recent PDL(λ) measurement results from the present system are presented in Fig. 9 for three artifacts. Only selected data points are shown along with the uncertainties calculated above and a least-squares fit to a fourth-order polynomial. These data span the PDL and wavelength range currently available for transfer via the NIST MAP.

VI. Conclusion

An accurate rapid nonmechanical technique of characterizing the wavelength dependence of polarization-dependent loss for both SM and bulk-optic devices has been developed that offers advantages over more traditional methods. The technique has an expanded uncertainty of $2u_{\mathrm{sys}} = 0.0098$ dB when measuring a device with 0.12 dB of PDL. A typical measurement scan requires 5 s. Overall accuracy is dependent on calibration to a primary artifact.

References

[1] M. Gadonna and A. Mabrouki, "Polarization sensitivity measurements methods for passive optical components," in *Proc. Conf. Eur. Fiber Optic Communications and Networks*, The Hague, Netherlands, 1993, pp. 65–67.

[2] Y. Zhu, E. Simova, P. Berini, and C. P. Grover, "A comparison of wavelength dependent polarization dependent loss measurements in fiber gratings," *IEEE Trans. Instum. Meas.*, vol. 49, pp. 1231–1239, Dec. 2000.

[3] R. M. Craig, S. L. Gilbert, and P. D. Hale, "High resolution, nonmechanical approach to polarization dependent transmission measurements," *J. Lightwave Technol.*, vol. 16, pp. 1285–1294, 1998.

[4] D. Derickson, Ed., *Fiber Optic Test and Measurement*. Englewood Cliffs, NJ: Prentice–Hall, 1998, ch. 9.5.

[5] B. M. Nyman, D. L. Favin, and G. Wolter, "System and method for measuring polarization dependent loss," in *OFC '94*, San Jose, CA, 1994, Tech. Dig., pp. –231.

[6] B. Nyman and G. Wolter, "High-resolution measurement of polarization dependent loss," *IEEE Photon. Technol. Lett.*, vol. 5, pp. 817–818, July 1993.

[7] S. L. Gilbert, W. C. Swann, and C. Wang, Hydrogen cyanide $H^{13}C^{14}N$ absorption reference for 1530 nm to 1560 nm wavelength calibration – SRM 2519, Special Pub. 260–137, Nat. Inst. Stand. Technol., Boulder, CO, 1998.

[8] B. N. Taylor and C. E. Kuyatt, Guidelines for evaluating and expressing the uncertainty of NIST measurement results, Tech. Note 1297, Nat. Inst. Stand. Technol., Boulder, CO, 1994.

[9] K. B. Rochford, A. H. Rose, P. A. Williams, C. M. Wang, I. G. Clarke, P. D. Hale, and G. W Day, "Design and performance of a stable linear retarder," *Appl. Opt.*, vol. 36, pp. 6458–6465, 1997.

R. M. Craig is a Physicist on the technical staff of the National Institute of Standards and Technology, Boulder, CO. He has been active there in radiometric and polarimetric metrology research since 1987. His professional interests include both fiber and bulk-optic polarimetry, polarimetric impairments to photonic devices and networks, as well as photonic network standards. He is also currently active in U.S. photonic network standards development and education.